Strength Behavior of High Strength R/C Columns under Biaxial Bending-Shear and Varying Axial Load

STRENGTH BEHAVIOR OF HIGH STRENGTH R/C COLUMNS UNDER

BIAXIAL BENDING-SHEAR AND VARYING AXIAL LOAD

Mitsuo MIZOGUCHI*, Takashi ARAKAWA and Yasuyuki ARAI*

ABSTRACT

Twelve short square R/C columns using high-strength concrete were tested to examine the effects of biaxial bending-shear force and varying axial load on the shear and flexural strength behavior. The columns were cyclically deflected either along their transverse principal axis to produce uniaxial bending-shear or along their diagonal to produce biaxial bending-shear. For columns failing in flexure, the experimental results were found to be in close agreement with the computed values given by the AIJ Code, regardless of the differences of concrete strength, biaxial bending-shear and varying axial load. For short columns subjected to low compressive or tensile axial stress, the computed ultimate shear strengths by the 1988 AIJ Design Equation overestimated the test results. The shear test results were in best agreement with the computed values by the "Kuramoto-Minami's Ultimate Shear Design Equation" proposed in 1990.

1. INTRODUCTION

Recently, there has been a rapid growth of demand for high-rise R/C buildings, which require the use of high-strength concrete and reinforcement. The experimental studies on the strength behavior of short R/C columns using high-strength materials has been carried out and published by many researchers[1,2]. On the other hand, in the case of square short columns with moderate levels of transverse reinforcement, it was pointed out in Ref. [9] that the previous loading in either direction did not significantly affect the ultimate shear strength of these columns. However, very few studies have been conducted on the flexural and shear strength behavior of high-strength concrete columns subjected to biaxial bending-shear and varying axial loads.

This report describes the test results (8 columns failing in shear and 4 columns failing in flexure) that examined the strength behavior of high-strength concrete (design strength Fc ranging from 300 to 600 kgf/cm²) columns under varying axial loads. In this test, specifically, two types of lateral loading along a principal axis to produce uniaxial bending-shear and lateral loading along a diagonal direction to produce biaxial bending-shear are applied and compared.

---

*Department of Civil Engineering and Architecture, Muroran Inst. of Tech.

2. EXPERIMENTAL PROGRAM

2.1 TEST SPECIMENS

A total of 12 approximately 1/5-scale column specimens shown in Fig.1 were tested. All specimens had an 18 cm square section with eight D13 longitudinal bars (gross reinforcement ratio Pg=3.14 %) and a clear height of column h_o=45 cm. Four specimens (transverse reinforcement ratio Pw=1.044 % and shear span ratio M/QD=2.5) were designed to fail in flexure and eight specimens (Pw=0.456 % and M/QD=1.25) were designed to fail in shear. The cross section of the test column was so decided to be able to produce a high axial compressive stress(σ_o=N/bD =150 kgf/cm²) when loaded by hydraulic actuator (capacity=50 tonf).
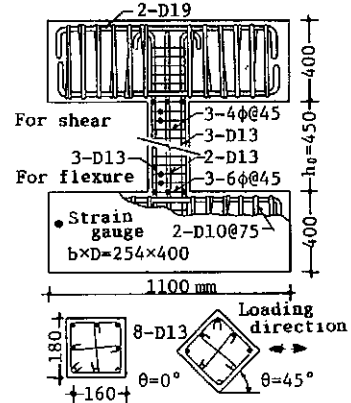

Fig.1 Details of specimen Test specimens

The specimens were named according to the loading condition and main variables as indicated in Table 1. The first numeral indicates the angle of loading with respect to the principal axis; 'O' is uniaxial lateral loading (θ=0°) and '4' is biaxial loading with diagonal load 45° from the principal axis. The second mark 'V' represents the varying axial load as shown in Fig.2 (b) and addition of 'f' represents the flexure test series. The third numerals '25','13' and '12' represent the fluctuating range of axial compressive stress ratio $\eta=\sigma_o/Fc$; the first '2' and '1' represent axial tension of η=-0.2 and η=-0.133 or -0.100, and the second '5', '3' and '2' represent axial compression of η=0.5, 0.33 and 0.25, respectively. The last marks 'ℓ', 'm' and 'h' are short for the design concrete strength of Fc=300, 450 and 600 kgf/cm².

Table 1

Fc kgf/cm²		Shear series I $\sigma_0 = -60 \sim 45 \sim 150$	Shear series II $\sigma_0 = -40 \sim 30 \sim 100$	Flexure series $\sigma_0 = -60 \sim 45 \sim 150$
300	n	$-0.200 \sim 0.150 \sim 0.500$	$-0.133 \sim 0.100 \sim 0.333$	
	2Q/3	-3.0 t 10.0t	-3.0 t 9.0t	
	$\theta= 0°$	OV25ℓ	OV13ℓ	
	$\theta=45°$	4V25ℓ	4V13ℓ	
450	n	$-0.133 \sim 0.100 \sim 0.333$		$-0.133 \sim 0.100 \sim 0.333$
	2Q/3	-3.0 t 12.0t		-1.5 t 7.0t
	$\theta= 0°$	OV13m		OV$_f$13m
	$\theta=45°$	4V13m		4V$_f$13m
600	n	$-0.100 \sim 0.075 \sim 0.250$		$-0.100 \sim 0.075 \sim 0.250$
	2Q/3	-3.0 t 14.0t		-1.5 t 7.0t
	$\theta= 0°$	OV12h		OV$_f$12h
	$\theta=45°$	4V12h		4V$_f$12h

2.2 LOADING HISTORY AND VARYING AXIAL LOAD

The horizontal load was applied by imposing a controlled deflection on the specimen. On the other hand, the applied axial load was given as a function of the horizontal load. As shown in Fig.2 (a), the deflection increment in each cycle was 0.9 mm (rotation angle R was defined as the lateral displacement δ divided by the clear height h_o, R=2x10⁻³=1/500 rad.) and the displacement was increased progressively from the beginning to the end of a total of 12 cycles (δ=10.8 mm, R=24x10⁻³≒1/40 rad.).

The axial load was varied proportional to the lateral shear force Q as shown in Fig.2(b). The values of σ_o= 30 and 45 kgf/cm² were assumed as the basic axial load stress of the column. The minimum and maximum axial loads were determined to develop as the lateral shear forces of column reached about 2/3 of the ultimate
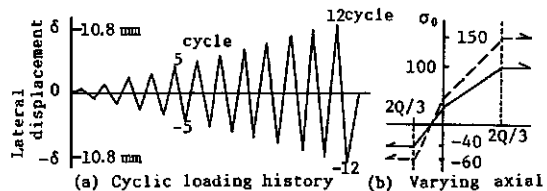

Fig.2 Cyclic loading history and varying axial load

shear strength calculated by the existing equation [3]. The values of 2Q/3 are shown in Table 1.

2.3 MATERIALS AND FABRICATION OF SPECIMENS

Properties of the reinforcing bars and the design concrete mix propor-tions are summarized in Table 2. All specimens were horizontally cast in steel forms. Three days after casting, the specimens and the control cylinders (diameter=10 cm and height =20 cm) were stripped, and then kept continuously wet and covered with a polyethylen sheet until 80 % of concrete design strength was attained. The specimens were tested at the age of 19~ 50 days. The actual concrete strengths of columns σ_B are given in Table 3.

Table 2 Materials

Reinforcement	Size	As (cm²)	σ_y (kgf/cm²)	E_S(x10⁶) (kgf/cm²)	Concrete	Fc (kgf/cm²)	w/c (%)	Mix.prop. C : S : G	Remark
	4φ	0.123	2070	1.974		300	60	1 : 2.86 : 3.73	for ℓ-type
	6φ	0.282	3770	2.050		450	44	1 : 2.24 : 3.58	OV13m, 4V13m
	D10	0.713	3870	—		450	42	1 : 2.88 : 3.76	OV$_f$13m, 4V$_f$13m
	D13	1.267	3500	1.840		600	31	1 : 1.75 : 2.73	for h-type
	D19	2.865	3870	—				by weight	

2.4 LOADING APPARATUS

Figure 3 shows an elevation view of the loading apparatus. Axial and lateral loads were applied to an L-shaped loading frames by hydraulic actuators ② and ③, respectively. Actuator ① was used for keeping the upper and lower loading beams hori-zontal during shear test. On the other hand, actuator ① was used for keeping such as the bending moment at the top of column M_{top}=0 and bending moment at the bottom M_{bot}= M_{max}. during flexure test.
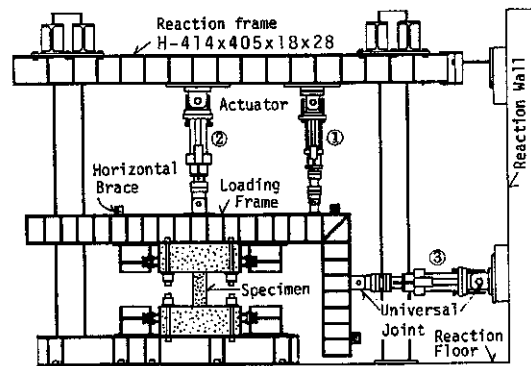

Fig.3 Loading apparatus

The influence of the angular deviation of vertical actuators on the lateral shear force was considered. Three horizontal braces were used for restraining the specimen from rotating in the direction normal to the load-ing plane during loading as shown by solid square marks in Fig.3.

2.5 INSTRUMENTATION AND TEST PROCEDURE

The applied lateral and axial loads were measured by load cells which were incorporated in the loading and restraining actuators ① to ③. In order to obtain the lateral displacement in the loading direction of column, four linear variable differential transducers were used, two on each side of the loading plane and located at the mid-depth of the upper and lower beams. Similarly, six linear transducers were used for measuring the axial dis-placements between the upper and lower beams. Strains in longitudinal and transverse reinforcement were measured by wire resistance strain gages (length=2 mm), as shown in Fig.1 by solid circle marks. Load—deflection curves and strains were recorded by personal computer and stored in floppy disk at each load stage. Also, crack patterns were traced and photographed.

3. TEST RESULTS AND DISCUSSION

3.1 FRACTURE PROCESSES

The applied axial load for a column is basically different between the positive and negative loading. Therefore, the crack pattern, failure mode and load-deflection relationship in each specimen are not symmetric as shown in Figs.4 and 5.
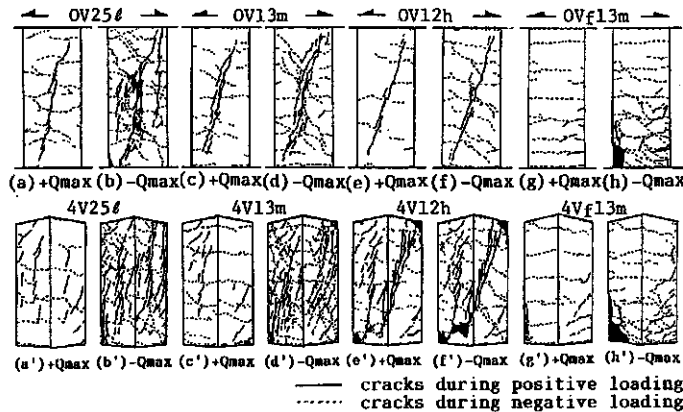

←— OV25ℓ —→   ←— OV13m —→   ←— OV12h —→   ←— OVf13m —→

(a)+Qmax (b)−Qmax(c)+Qmax(d)−Qmax(e)+Qmax (f)−Qmax (g)+Qmax(h)−Qmax

4V25ℓ   4V13m   4V12h   4Vf13m

(a')+Qmax (b')−Qmax (c')+Qmax (d')−Qmax (e')+Qmax (f')−Qmax (g')+Qmax (h')−Qmax

——— cracks during positive loading
······· cracks during negative loading

Fig.4 Cracking pattern and after failure

Fig.5 Load-displacement envelope curves

(1) Shear test series

In the positive loading of the OV-type column, flexural cracks occured in the first cycle at both ends of the column. And then the diagonal cracks appeared in the 2nd~3rd cycles as shown in Figs.4 (a), (c) and (e). Soon after that, these shear cracks extended and a little bit widened. The maximum lateral loads were reached after yielding of the transverse reinforcements placed at the position of 9 cm from both ends of the column. In the case of high-strength concrete columns, it was observed that few cracks appeared and the load carrying capacities dropped rapidly after reaching maximum load.

In the negative loading of the OV-type column, the crack appearance and its propagation behavior are different from those of the positive loading, because the applied axial load of column varied from compression to tension. The shear cracks were more horizontally inclined and widely distributed throughout the height of the column than those in case of the positive loading. These shear cracks extended with the increase in the displacement level and crossed with the diagonal shear cracks of the positive loading. With further increase in loading cycles, the maximum loads were attained with spalling of cover concrete on the longitudinal middle bars. The load carrying capacity of column reduced gradually as shown in Figs.5 (a) and (b).

On the other hand, for the diagonally loaded 4V-type columns, the cracks widely propagated on all face of column. The crack propagation and transverse reinforcement yielding in the both positive and negative loading were similar to the OV-type columns.

(2) Flexure test series

In the positive loading, all four columns reached the maximum load at the 4th~5th cycles and failed in flexure with the longitudinal bars yielded
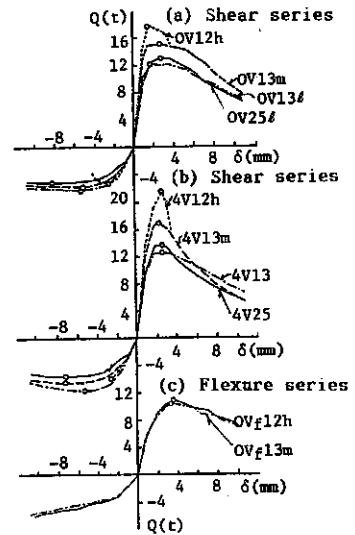
and concrete crushed, in spite of differences of concrete strength and lateral loading direction angle θ.

In the negative loading under axial tension, the load carrying capacity of the column increased gradually with the increase in loading cycles. The cyclic loading was stopped at the 12th cycle leaving a reserve tensile strength.

(3) Load-displacement envelope curves

In the positive loading of the shear test series, as shown in Figs.5 (a) and (b), the ultimate shear strength is higher for columns with higher concrete strength σ_B.   However, the load carrying capacity after reaching maximum load dropped rapidly. This tendency is more remarkable in the 4V-type columns than the OV-type columns.

On the other hand, in the negative loading, no recognizable differences with respect to σ_B and θ were observed. The load carrying capacity after reaching maximum load showed a smoother slope.

In the case of the flexure test series as shown in Fig.5 (c), the slope of load carrying capacity after reaching maximum load was more gentle than the shear test series.

3.2 CRACKING STRENGTH

(1) Flexural cracking load

Figure 6 shows the results of the influence of σ_B on the flexural cracking load. In this figure, the three dotted lines show computed values given by Eq.(1) assuming that axial stress σ_0=0 and 150 kgf/cm². As can be seen, all the test results in the positive loading show a little higher values than the computed values (as a square column) obtained from Eq.(1),   To the contrary, in the negative loading, test results are a little lower than the computed values. However, the test results   resembled with the tendency of Eq.(1).

Fig.6 Flexural cracking load

Fig.7 Shear cracking load

(2) Shear cracking load

As shown in Fig.7, the shear cracking loads in the both positive and negative loading increase a little in proportion to the increase of concrete strength σ_B. The existing empirical Eq.(2) for shear cracking strength can be applied to the high strength concrete columns under biaxial bending-shear and varying axial load.

3.3 ULTIMATE STRENGTH

The ultimate shear and flexural strengths of column subjected to varying axial load can be evaluated by adopting the lateral shear forces $_tQ_u$ as the axial load reached maximum in each positive and negative loading.   The measured $_tQ_u$ and the ratios of the test results to the computed values by Eqs.(1) ~ (5) are listed in Table 3.
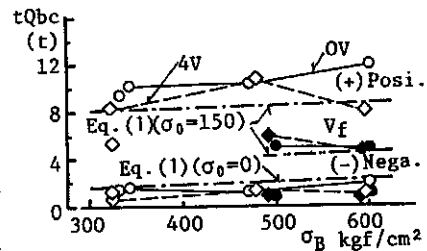
Table 3   Test results
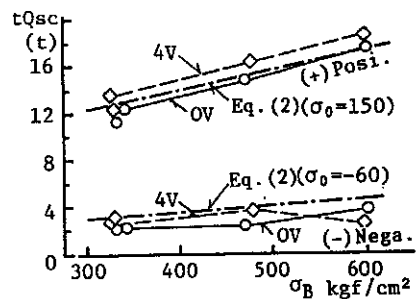
Column No.	σB, σt (kgf/cm²)	Loading	At flexural cracking			At shear cracking			At maximum load						Failure mode
			η	tQbc (ton)	tQbc/cQbc	η	tQsc (ton)	tQsc/cQsc	η	tQu (ton)	tδu (mm)	tQu/cQsu	tQu/cQs	tQu/cQfu	
OV25ℓ	342 / 31.0	+	0.439	10.30	1.24	0.438	12.40	1.07	0.439	13.04	2.72	0.84	1.02	0.78	S
		–	-0.023	1.54	0.93	-0.090	2.09	0.45	-0.175	5.21	8.12	0.69	0.88	0.55	S
OV13ℓ	332 / 33.3	+	0.299	9.49	1.56	0.300	11.43	1.20	0.301	12.24	1.69	0.91	0.98	0.71	S
		–	0.003	1.24	0.60	-0.061	2.07	0.42	-0.120	6.35	5.42	0.78	0.82	0.37	S
OV13m	471 / 41.9	+	0.290	10.49	1.31	0.316	14.89	1.12	0.318	15.22	2.70	0.86	0.91	0.71	S
		–	0.032	1.25	0.45	-0.078	2.34	0.46	-0.127	5.83	5.16	0.62	0.97	0.34	S
OV12h	602 / 52.3	+	0.225	12.03	1.48	0.248	17.64	1.16	0.249	17.76	1.47	0.90	0.88	0.78	S
		–	-0.035	1.90	1.37	-0.100	3.95	0.87	-0.100	5.29	2.66	0.46	0.87	0.35	S
4V25ℓ	323 / 30.4	+	0.409	8.36	1.12	0.468	13.68	1.21	0.464	13.83	2.71	0.91	1.13	0.88	S
		–	0.016	1.20	0.60	-0.152	2.07	0.71	-0.186	5.45	7.20	0.75	0.93	0.37	S
4V13ℓ	328 / 30.5	+	0.217	5.36	1.10	0.305	12.45	1.31	0.305	12.64	2.66	0.94	1.02	0.73	S
		–	0.032	0.89	0.40	-0.123	3.23	0.77	-0.122	7.52	5.41	0.93	0.97	0.59	S
4V13m	478 / 41.4	+	0.295	10.94	1.34	0.313	16.17	1.20	0.314	17.08	2.32	0.96	1.00	0.79	S
		–	-0.007	1.41	0.72	-0.126	3.81	0.95	-0.126	6.35	7.22	0.66	1.05	0.42	S
4V12h	598 / 51.3	+	0.176	8.10	1.18	0.251	19.00	1.25	0.251	21.64	2.66	1.10	1.07	0.95	S
		–	0.001	1.29	0.55	-0.080	2.53	0.49	-0.100	5.85	2.69	0.52	0.96	0.38	S
OVf13m	509 / 43.3	+	0.235	5.00	1.37	—	—	—	0.295	10.90	3.62	0.79	0.60	0.99	F
		–	0.013	0.79	0.65	—	—	—	-0.118	>5.85	10.47	0.77	0.49	0.91	F
OVf12h	603 / 49.8	+	0.197	4.97	1.34	0.247	9.69	0.93	0.249	10.43	3.32	0.72	0.54	0.91	F
		–	-0.036	0.96	1.39	—	—	—	-0.100	>5.59	10.87	0.67	0.46	0.87	F
4Vf13m	492 / 42.1	+	0.279	6.10	1.52	0.302	8.96	0.96	0.305	9.77	4.32	0.72	0.54	0.90	F
		–	-0.028	0.90	1.20	—	—	—	-0.122	>5.85	10.32	0.79	0.47	0.91	F
4Vf12h	598 / 47.6	+	0.195	4.80	1.31	—	—	—	0.250	10.69	3.56	0.74	0.55	0.94	F
		–	-0.022	0.94	1.08	—	—	—	-0.100	>6.12	10.81	0.74	0.51	0.95	F

For the calculation of the shear force Q in the following equations, the differences of loading direction angle θ are neglected.

Flexural cracking strength [3]:

$$M_{bc}=1.8\sqrt{\sigma_B}\cdot Ze + ND/6, \qquad cQ_{bc}=\Sigma M_{bc}/h_o \quad \cdots\cdots\cdots(1)$$

Shear cracking strength [3]:

$$Q_{sc}=\{0.085kc(\sigma_B+500)/(M/Qd+1.7)\}bj, \qquad cQ_{sc}=(1+\sigma_o/150)Q_{sc}\cdots\cdots(2)$$

Ultimate shear strength [3]:

$$Q_{su}=\{0.115kukp(\sigma_B+180)/(M/Qd+0.12) + 2.7\sqrt{Pw\sigma wy}\}bj,$$
$$cQ_{su}=(0.9+\sigma_o/250)Q_{su}, \qquad (\sigma_o\leqq150) \quad \cdots\cdots\cdots\cdots(3)$$

Kuramoto-Minami's equation [4]:

$$cQs=bd\cdot Pw\sigma wy + (\gamma-2\alpha\cdot Pw\sigma wy/\sigma_B)bD\sigma_B\cdots\cdots\cdots\cdots\cdots\cdots(4)$$
$$\text{as } \eta\leqq0.5-2q, \quad \gamma=\{\sqrt{4(\eta+2q)(1-\eta-2q)+(L/D)^2}-(L/D)\}/2,$$
$$\text{as } \eta>0.5-2q, \quad \gamma=\alpha=(\sqrt{1+(L/D)^2}-(L/D))/2$$

Ultimate flexural strength [3]:

$$Nmax\geqq N>Nb, \quad Mu=\{0.5a_g\sigma_yg_1D+0.024(1+g_1)(3.6-g_1)bD^2\sigma_B\}$$
$$\times(Nmax-N)/(Nmax-N_b)$$
$$N_b\geqq N>0, \quad Mu=0.5a_g\sigma_yg_1D+0.5ND(1-N/bD\sigma_B)$$
$$0>N\geqq Nmin, \quad Mu=0.5a_g\sigma_yg_1D+0.5Ng_1D, \qquad cQfu=\Sigma Mu/h_o\cdots\cdots\cdots(5)$$

(1) Ultimate shear strength

Figure 8 shows a relationship between $_tQ_u$ and σ_B. In this figure, the dotted lines are the computed values of a square column given by Eqs.(3) and (4) assuming that $\sigma_o=$ 150, -60 kgf/cm² and neglecting the effect of θ. Also, the computed values obtained from 1988 AIJ Design Equation and AIJ R/C Standard [5,6] are shown by broken lines.

As can be seen, the $_tQ_u$ in the positive loading increased in proportion to the σ_B. The rate of increase
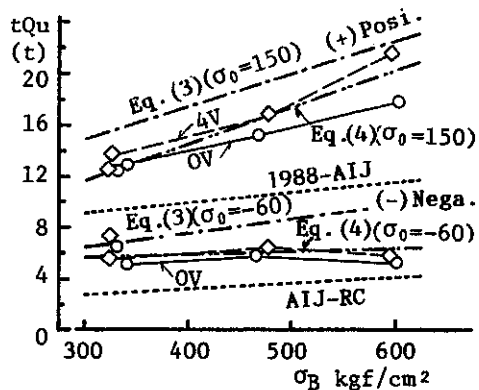

Fig.8 Ultimate shear strength

in 4V-type columns are a little higher than that of 0V-type columns.

In comparison with the 25ℓ-type and 13ℓ-type columns under same σ_B but having different fluctuating range of η, as shown in Table 3, the $_tQ_u$ of 25ℓ-type columns with high η indicated a little higher value than that of the 13ℓ-type columns. On the other hand, in case of the 13ℓ-type and 13m-type columns under same fluctuating range of η but having different σ_B, the $_tQ_u$ of 13m-type columns with high σ_B indicated a little higher value than that of the 13ℓ-type columns.

(2) Comparison of the shear test results with computed values

In the positive loading, the shear test results are about 16 % lower than the computed values given by the existing Eq.(3). This means that the Eq.(3) overestimated the test results. But the results are in best agreement with the computed values obtained from "Ultimate Shear Strength Eq.(4)" proposed by Kuramoto-Minami in 1990, regardless of the differences of loading direction and varying axial load. In this case, it is necessary to expand the applicable upper limit of σ_B up to 600 kgf/cm².

In the negative loading, the shear test results showed almost constant values regardless of the differences of σ_B and θ, and are in best agreement with the computed values given by Eq.(4).

For the allowable temporary shear force of column prescribed in the "AIJ R/C Standard" [6], all shear test results in the both of positive and negative loading are conservative values. However, it is necessary to note that the "1988 AIJ Design Equation" [5] and Eq.(3) overestimate the shear forces of the columns with tensile axial stress.

(3) Flexure test results

As listed in Table 3, flexural strength of four columns in the positive loading showed almost all same values, in spite of differences of θ and σ_B. These test results are in good agreement with the computed values given by the flexural strength Eq.(5). On the other hand, in the negative loading under axial tension, the cyclic loading was stopped at about 90% of computed values given by Eq.(5).

(4) Comparison of the past shear tests with computed values

Table 4 shows a comparison of the past shear data of 32 columns tested in our laboratory [7,8] with the computed values given by Eqs.(3),(4) and AIJ Commentary Eq.(6.9) [5]. For the 18 columns in the Ref.[8] and this test, because the axial loads in the positive and negative loadings are different, the data in both loadings are treated separately. Therefore, a total of 50 sets of test results data were compared.

As listed in Table 4, the computed values given by Eq.(3) are a little overestimated. On the contrary, the values by Eq.(6.9) are a little underestimated.

Table 4   Comparison of shear test data with computed values

Data	Axial load	No.	Eq.(3)			AIJ Com.Eq.(6.9)			Eq.(4)		
			$\frac{tQu}{cQsu}$	Standard devi.	Varia. ratio%	$\frac{tQu}{cVu}$	Standard devi.	Varia. ratio%	$\frac{tQu}{cQs}$	Standard devi.	Varia. ratio%
Ref.7 14	Compr.	9	0.94	0.085	8.8	1.15	0.093	8.1	1.13	0.091	8.0
	0-Ten.	5	0.98	0.093	9.5	0.98	0.050	5.1	0.96	0.050	5.2
Ref.8 10	Compr.	10	0.91	0.046	5.0	1.15	0.055	4.8	1.11	0.051	4.6
	0-Ten.	10	0.97	0.065	6.8	0.86	0.061	7.1	0.82	0.059	7.1
Herein 8	Compr.	8	0.93	0.074	8.0	1.18	0.115	9.8	1.00	0.078	7.8
	Ten.	8	0.68	0.138	20.5	1.42	0.140	9.8	0.93	0.068	7.3
Total 32	Comp.	27	0.93	0.073	7.8	1.16	0.090	7.7	1.08	0.092	8.4
	0-Ten.	23	0.87	0.173	20.0	1.08	0.268	24.8	0.89	0.085	9.6
	Total	50	0.90	0.133	14.8	1.12	0.197	17.5	0.99	0.131	13.2

Figure 9 shows the relationship between the ratio of the test results to the computed values given by Eq.(4) and the axial compressive stress ratio η . The ratios of $_tQ_u/_cQ_s$ showed a tendency to slightly increase in proportion to η . However, the average ratio taken from the 50 data sets is equal to 0.99 (standard deviation is 0.131 and variation rate is 13.2 %). Also, the computed values by Eq.(4) are in best agreement with test results.
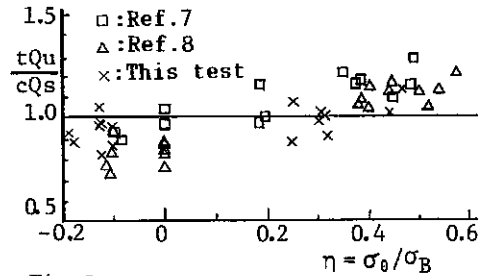

Fig.9 Comparison of $_tQ_u/_cQ_s$ and η

4. CONCLUSION

Based on the results of this study the following conclusions were made:
(1) The ultimate shear strength of short column, within the range of $\sigma_B=300 \sim 600$ kgf/cm^2, increases in proportion to the concrete strength σ_B.
(2) The ultimate shear and flexural strength of short column under biaxial bending-shear is similar to that of column loaded along the principal axis and there is almost no need to consider the effect of θ .
(3) The ultimate shear and flexural strength of short column under varying axial load can be evaluated by adopting the lateral shear force as the axial load reached to maximum in each positive and negative loading.
(4) The computed value obtained from Eq.(4) proposed by Kuramoto-Minami is in best agreement with the shear test results. It is necessary to note that the 1988 AIJ Design Equation and Eq.(3) overestimate the calculated values as compared to the test results for the short column under tensile axial stress.

ACKNOWLEDGEMENT

REFERENCES

[1] Tanaka,R.,et al, "Some Special Aspects to be Considered in Designing Reinforced Concrete Structural Members with High Strength Reinforcements," Concrete Journal,Vol.28,No.4,Apr.1990,pp.37-43, No.5,May,1990, pp.41-48, No.6,June,1990,pp.16-23.(in Japanese).
[2] AIJ,"State-of-the-Art Report on High-Strength Concrete," 1991.(in Jap.)
[3] AIJ,"Data for Ultimate Strength Design of Reinforced Concrete Structures," 1987,pp.112-129.(in Japanese).
[4] Kuramoto,H. and Minami,K.,"Ultimate Shear Design Equations for R/C Members Applying Plasticity," Trans. of AIJ No.417, Journalof Structural and Construction Eng.,1990, pp.31-45.(in Japanese).
[5] AIJ,"Design Guideline for Earthquake Resistant R/C Buildings Based on Ultimate Strength Concept," 1988,pp.112-129.(in Japanese).
[6] AIJ,"AIJ Standard for Structural Calculation of Reinforced Concrete Structures,"1985,pp.32-37.
[7] Arakawa,T.,et al,"Shear Resisting Behavior of Short R/C Columns under Biaxial Bending-Shear,"Trans. of JCI,Vol.11,1989,pp.317-324.
[8] Mizoguchi,M.,et al,"Shear Resisting Behavior of Short R/C Columns under Biaxial Bending-Shear and Varying Axial Load,"Trans. of JCI,Vol.12,1990, pp.347-354.
[9] Maruyama,K., Ramirez,H. and Jirsa,J.O.,"Short RC Columns Under Bilateral Load Histories," ASCE,Journal of S.E.,Vol.110, No.1,1984,pp.120-137.